
A Generic Approach for Escaping Saddle points

Anonymous Author(s)

Affiliation

Address

email

Abstract

1 A central challenge to using first-order methods for optimizing nonconvex problems is
2 the presence of saddle points. First-order methods often get stuck at saddle points, greatly
3 deteriorating their performance. Typically, to escape from saddles one has to use second-
4 order methods. However, most works on second-order methods rely extensively on expensive
5 Hessian-based computations, making them impractical in large-scale settings. To tackle this
6 challenge, we introduce a generic framework that minimizes Hessian based computations
7 while at the same time provably converging to second-order critical points. Our framework
8 carefully alternates between a first-order and a second-order subroutine, using the latter only
9 close to saddle points, and yields convergence results competitive to the state-of-the-art.
10 Empirical results suggest that our strategy also enjoys good practical performance.

11 1 Introduction

12 We study nonconvex *finite-sum* problems of the form

$$\min_{x \in \mathbb{R}^d} f(x) := \frac{1}{n} \sum_{i=1}^n f_i(x), \quad (1)$$

13 where $f : \mathbb{R}^d \rightarrow \mathbb{R}$ nor the individual functions $f_i : \mathbb{R}^d \rightarrow \mathbb{R}$ ($i \in [n]$) are necessarily convex. Optimization
14 problems of this form arise naturally in machine learning e.g. empirical risk minimization.

15 In the large-scale settings, algorithms based on first-order information of functions f_i are typically favored
16 as they are relatively inexpensive and scale seamlessly. An algorithm widely used in practice is stochastic
17 gradient descent (SGD) which under suitable selection of the learning rate converges to a point x that, in
18 expectation, satisfies the stationarity condition $\|\nabla f(x)\| \leq \epsilon$ in $O(1/\epsilon^4)$ iterations [9]. This result neither
19 ensures convergence to second-order critical points nor the rate is fast. For general nonconvex problems, one
20 has to settle for a more modest goal than sub-optimality, as finding the global minimizer is intractably hard.
21 Unfortunately, SGD does not even ensure second-order critical conditions as it can get stuck at saddle points.

22 To overcome these issues, the cubic regularization (CR) method [23] explicitly uses Hessians to obtain faster
23 convergence rates. In particular, Nesterov and Polyak [23] showed that CR requires $O(1/\epsilon^{3/2})$ iterations
24 to achieve the second-order critical conditions. However, each iteration of CR is expensive as it requires
25 computing the Hessian and solving multiple linear systems, each of which has complexity $O(d^\omega)$ (ω is the
26 matrix multiplication constant), thus, undermining the benefit of its faster convergence. Recently, Agarwal
27 et al. [2] designed an algorithm to solve the CR more efficiently, however, it still exhibits slower convergence
28 in practice compared to first-order methods. Both of these approaches use Hessian based optimization in each
29 iteration, which make them slow in practice.

30 A second line of work focuses on using Hessian information (or its structure) whenever the method gets stuck
31 at stationary points that are not second-order critical. To our knowledge, the first work in this line is [8], which
32 shows that for a class of functions that satisfy a special property called “strict-saddle” property, a noisy variant
33 of SGD can converge to a point close to a local minimum. For this class of functions, points close to saddle
34 points have a Hessian with a large negative eigenvalue, which proves instrumental in escaping saddle points
35 using an isotropic noise. While such a noise-based method is appealing as it only uses first-order information,
36 it has a very bad dependence on the dimension d , and furthermore, the result only holds when the strict-saddle
37 property is satisfied [8].

38 Inspired by this line of work, we develop a general framework for finding second-order critical points. The
39 key idea is to use first-order information for the most part of the optimization process and invoke Hessian
40 information only when stuck at stationary points that are not second-order critical.

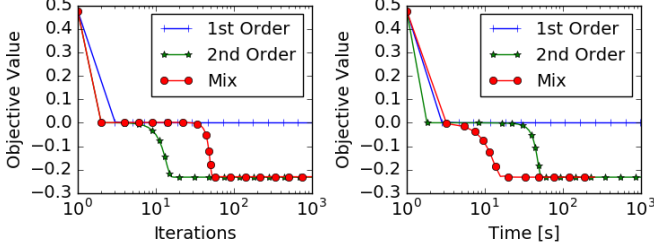


Figure 1: First order methods like GD can potentially get stuck at saddle points. Second-order methods can escape it in very few iterations (as observed in the left plot) but at the cost of expensive Hessian based iterations (see time plot to the right). The proposed framework, which is a novel mix of the two strategies, can escape saddle points *faster* in time by carefully trading off computation and iteration complexity.

2 Background & Problem Setup

We assume that each of the functions f_i in (1) is L -smooth, i.e., $\|\nabla f_i(x) - \nabla f_i(y)\| \leq L\|x - y\|$ for all $i \in [n]$. Furthermore, we assume that the Hessian of f in (1) is M -Lipschitz, i.e., $\|\nabla^2 f(x) - \nabla^2 f(y)\| \leq M\|x - y\|$ for all $x, y \in \mathbb{R}^d$. We also assume that the function f is bounded below, i.e., $f(x) \geq B$ for all $x \in \mathbb{R}^d$.

In order to measure stationarity of an iterate x , similar to [9, 22, 23], we use the condition $\|\nabla f(x)\| \leq \epsilon$. In this paper, we are interested in convergence to second-order critical points. Thus, in addition to stationarity, we also require the solution to satisfy the Hessian condition $\nabla^2 f(x) \succeq -\gamma\mathbb{I}$ [23].

Definition 1. An algorithm \mathcal{A} is said to obtain a point x that is a (ϵ, γ) -second order critical point if $\mathbb{E}[\|\nabla f(x)\|] \leq \epsilon$ and $\mathbb{E}[\nabla^2 f(x)] \succeq -\gamma\mathbb{I}$, where the expectation is over any randomness in \mathcal{A} .

For our algorithms, we use only cheap Incremental First-order Oracle (IFO) [1] and an Incremental Second-order Oracle (ISO), which have time complexity $O(d)$ in many practical settings.

Definition 2. An IFO takes an index $i \in [n]$ and a point $x \in \mathbb{R}^d$, and returns the pair $(f_i(x), \nabla f_i(x))$. An ISO takes an index $i \in [n]$, point $x \in \mathbb{R}^d$ and vector $v \in \mathbb{R}^d$ and returns the vector $\nabla^2 f_i(x)v$.

For clarity and clean comparison, the dependence of time complexity on Lipschitz constant L , M , initial point and any polylog factors in the results is hidden.

3 Generic Framework

We propose a generic framework for escaping saddle points while solving nonconvex problems of form (1). To evade saddle points, one needs to use properties of both gradients and Hessians. To this end, our framework is based on two core subroutines: GRADIENT-FOCUSED-OPTIMIZER and HESSIAN-FOCUSED-OPTIMIZER.

The idea is to use these two subroutines, each focused on different aspects of the optimization procedure. GRADIENT-FOCUSED-OPTIMIZER focuses on using gradient information for decreasing the function. On its own, the GRADIENT-FOCUSED-OPTIMIZER might not converge to a second order critical point since it can get stuck at a saddle point. Hence, we require the subroutine HESSIAN-FOCUSED-OPTIMIZER to help avoid saddle points. We design a procedure that interleaves these subroutines to obtain a second-order critical point, which not only provides meaningful theoretical guarantees, but also translates into strong empirical gains.

Algorithm 1 provides pseudocode of our framework. Observe that the algorithm is still abstract, and we assume the following properties to hold for these subroutines.

- **GRADIENT-FOCUSED-OPTIMIZER:** Suppose $(y, z) = \text{GRADIENT-FOCUSED-OPTIMIZER}(x, n, \epsilon)$, then there exists positive function $g : \mathbb{N} \times \mathbb{R}^+ \rightarrow \mathbb{R}^+$, such that

G.1 $\mathbb{E}[f(y)] \leq f(x)$,

G.2 $\mathbb{E}[\|\nabla f(y)\|^2] \leq \frac{1}{g(n, \epsilon)} \mathbb{E}[f(x) - f(z)]$.

Here the outputs $y, z \in \mathbb{R}^d$. The expectation in the conditions above is over any randomness that is a part of the subroutine. The function g will be critical for the overall rate of Algorithm 1. Typically, GRADIENT-FOCUSED-OPTIMIZER is a first-order method, since the primary aim of this subroutine is to focus on gradient based optimization.

- **HESSIAN-FOCUSED-OPTIMIZER:** Suppose $(y, \tau) = \text{HESSIAN-FOCUSED-OPTIMIZER}(x, n, \epsilon, \gamma)$ where $y \in \mathbb{R}^d$ and $\tau \in \{\emptyset, \diamond\}$. If $\tau = \emptyset$, then y is a (ϵ, γ) -second order critical point with probability at least $1 - q$. Otherwise if $\tau = \diamond$, then y satisfies the following condition:

H.1 $\mathbb{E}[f(y)] \leq f(x)$,

H.2 $\mathbb{E}[f(y)] \leq f(x) - h(n, \epsilon, \gamma)$ when $\lambda_{\min}(\nabla^2 f(x)) \leq -\gamma$ for some $h : \mathbb{N} \times \mathbb{R}^+ \times \mathbb{R}^+ \rightarrow \mathbb{R}^+$.

Here the expectation is over any randomness in subroutine. The two conditions ensure that the objective function value, in expectation, never increases and decreases with a certain rate when $\lambda_{\min}(\nabla^2 f(x)) \leq -\gamma$. In general, this subroutine utilizes the Hessian or its properties for minimizing the objective function. Typically, this is the most expensive part of the Algorithm 1 and hence, needs to be invoked judiciously.

Algorithm 1 Generic Framework

```

1: Input - Initial point:  $x^0$ , total iterations  $T$ , error threshold parameters  $\epsilon, \gamma$  and probability  $p$ 
2: for  $t = 1$  to  $T$  do
3:    $(y^t, z^t) = \text{GRADIENT-FOCUSED-OPTIMIZER}(x^{t-1}, \epsilon)$  (refer to G.1 and G.2)
4:   Choose  $u^t$  as  $y^t$  with probability  $p$  and  $z^t$  with probability  $1 - p$ 
5:    $(x^{t+1}, \tau^{t+1}) = \text{HESSIAN-FOCUSED-OPTIMIZER}(u^t, \epsilon, \gamma)$  (refer to H.1 and H.2)
6:   if  $\tau^{t+1} = \emptyset$  then
7:     Output set  $\{x^{t+1}\}$ 
8:   end if
9: end for
10: Output set  $\{y^1, \dots, y^T\}$ 

```

3.1 Convergence Analysis

The key aspect of these subroutines is that they, in expectation, never increase the objective function value. The functions g and h will determine the convergence rate of Algorithm 1.

Theorem 1. *Let $\Delta = f(x^0) - B$ and $\theta = \min((1 - p)\epsilon^2 g(n, \epsilon), ph(n, \epsilon, \gamma))$. Also, let set Γ be the output of Algorithm 1 with GRADIENT-FOCUSED-OPTIMIZER satisfying **G.1** and **G.2** and HESSIAN-FOCUSED-OPTIMIZER satisfying **H.1** and **H.2**. Furthermore, T be such that $T > \Delta/\theta$. Suppose the multiset $S = \{i_1, \dots, i_k\}$ are k indices selected independently and uniformly randomly from $\{1, \dots, |\Gamma|\}$. Then the following holds for the indices in S :*

1. y^t , where $t \in \{i_1, \dots, i_k\}$, is a (ϵ, γ) -critical point with probability at least $1 - \max(\Delta/(T\theta), q)$.
2. If $k = O(\log(1/\zeta)/\min(\log(\Delta/(T\theta)), \log(1/q)))$, with at least probability $1 - \zeta$, at least one iterate y^t where $t \in \{i_1, \dots, i_k\}$ is a (ϵ, γ) -critical point.

The proof of the result is presented in Appendix B. The key point regarding the above result is that the overall convergence rate depends on the magnitude of both functions g and h . Theorem 1 shows that the slowest amongst the subroutines GRADIENT-FOCUSED-OPTIMIZER and HESSIAN-FOCUSED-OPTIMIZER governs the overall rate of Algorithm 1. Thus, it is important to ensure that both these procedures have good convergence. Also, note that the optimal setting for p based on the result above satisfies $1/p = 1/\epsilon^2 g(n, \epsilon) + 1/h(n, \epsilon, \gamma)$.

3.2 An Example Instantiation

We now present a specific instantiation of our framework and derive the time complexity required to reach a second order critical point. For this example we use SVRG as the GRADIENT-FOCUSED-OPTIMIZER and HESSIANDESCENT as the HESSIAN-FOCUSED-OPTIMIZER.

- SVRG [12, 26] is a stochastic algorithm recently shown to be very effective for reducing variance in finite-sum problems. Strong convergence rates have been proved for SVRG in the context of convex and nonconvex optimization [12, 26]. The following result shows that SVRG meets the requirements of a GRADIENT-FOCUSED-OPTIMIZER.

Lemma 1. SVRG with $\eta_t = \eta = 1/4Ln^{2/3}$, $m = n$ and $T_g = T_\epsilon$, which depends on ϵ , is a GRADIENT-FOCUSED-OPTIMIZER with $g(n, \epsilon) = T_\epsilon/40Ln^{2/3}$.

The algorithm for SVRG and the proof of the result is presented in Appendix C.

- HESSIANDESCENT is a direct approach using the eigenvector corresponding to the smallest eigenvalue of the hessian to make a descent step. More specifically, when the smallest eigenvalue of the Hessian is negative and reasonably large in magnitude, i.e. $\lambda_{\min}(\nabla^2 f(x)) \leq -\gamma$ then the Hessian information can be used to ensure descent in the objective function value. Note the subroutine is designed in a fashion such that the objective function value never increases. The following result shows that HESSIANDESCENT meets the requirements of a HESSIAN-FOCUSED-OPTIMIZER.

Lemma 2. HESSIANDESCENT is a HESSIAN-FOCUSED-OPTIMIZER with $h(n, \epsilon, \gamma) = \frac{\rho}{24M^2} \gamma^3$.

The algorithm for HESSIANDESCENT and proof of the result is presented in Appendix D.

Now we can show the following key result:

Theorem 2. *Suppose SVRG with $m = n$, $\eta_t = \eta = 1/4Ln^{2/3}$ for all $t \in \{1, \dots, m\}$ and $T_g = 40Ln^{2/3}/\epsilon^{1/2}$ is used as GRADIENT-FOCUSED-OPTIMIZER and HESSIANDESCENT is used as HESSIAN-FOCUSED-OPTIMIZER with $q = 0$, then Algorithm 1 finds a $(\epsilon, \sqrt{\epsilon})$ -second order critical point in $T = O(\Delta/\min(p, 1 - p)\epsilon^{3/2})$ with probability at least 0.9.*

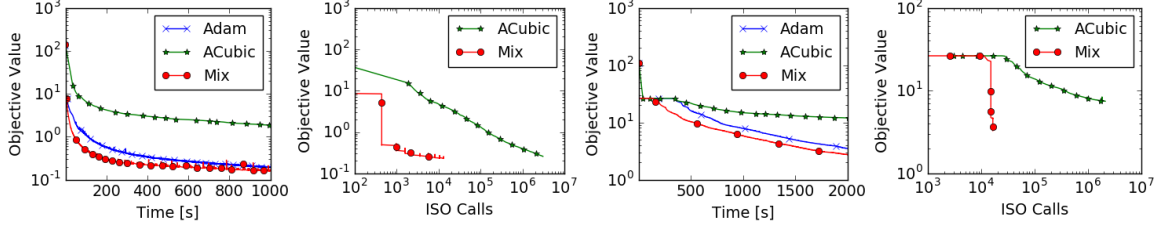


Figure 2: Comparison of various methods on CURVES and MNIST Deep Autoencoder. Our mix approach converges faster than the baseline methods and uses relatively few ISO calls, which are practically relatively expensive to IFO calls, in comparison to APPROXCUBICDESCENT.

125 The result directly follows from using Lemma 1 and 2 in Theorem 1. Combining this with the time
 126 complexity of SVRG which is $O(nd + T_g d) = O(nd + n^{2/3}d/\epsilon^{1/2})$ and HESSIANDESCENT which is
 127 $(O(nd + n^{3/4}d/\epsilon^{1/4}))$, we get the following result.

128 **Corollary 1.** *The overall running time of Algorithm 1 to find a $(\epsilon, \sqrt{\epsilon})$ -second order critical point, with*
 129 *parameter settings used in Theorem 2, is $O(nd/\epsilon^{3/2} + n^{3/4}d/\epsilon^{7/4} + n^{2/3}d/\epsilon^2)$.*

130 Note that the dependence on ϵ is much better in comparison to that of Noisy SGD used in [8]. Furthermore, our
 131 results are competitive with [2, 4] in their respective settings, but with a much simpler algorithm and analysis.
 132 We also note that our algorithm is faster than [11], which has a time complexity of $O(nd/\epsilon^2)$.

133 3.3 Practical Considerations

134 To further achieve good empirical performance, we had to slightly modify these procedures. For
 135 HESSIAN-FOCUSED-OPTIMIZER, we found stochastic, adaptive and inexact approaches for solving
 136 HESSIANDESCENT and CUBICDESCENT work well in practice. Due to lack of space, the exact description of
 137 these modifications is deferred to Appendix F. Furthermore, in the context of deep learning, empirical evidence
 138 suggests that first-order methods like ADAM [13] exhibit behavior that is in congruence with properties G.1
 139 and G.2. While theoretical analysis for a setting where ADAM is used as GRADIENT-FOCUSED-OPTIMIZER
 140 is still unresolved, we nevertheless demonstrate its performance through empirical results.

141 4 Experiments

142 To investigate the practical performance of the framework, we applied it to two deep autoencoder optimization
 143 problems from [10] called “CURVES” and “MNIST”. Due to their high difficulty, performance on these
 144 problems has become a standard benchmark for neural network optimization methods, e.g. [20, 21, 32, 33].
 145 The “CURVES” autoencoder consists of an encoder with layers of size (28x28)-400-200-100- 50-25-6 and a
 146 symmetric decoder totaling in 0.85M parameters. The six units in the code layer were linear and all the other
 147 units were logistic. The network was trained on 20,000 images and tested on 10,000 new images. The data set
 148 contains images of curves that were generated from three randomly chosen points in two dimensions. The
 149 “MNIST” autoencoder consists of an encoder with layers of size (28x28)-1000-500-250-30 and a symmetric
 150 decoder, totaling in 2.8M parameters. The thirty units in the code layer were linear and all the other units were
 151 logistic. The network was trained on 60,000 images and tested on 10,000 new images. The data set contains
 152 images of handwritten digits 0-9. The pixel intensities were normalized to lie between 0 and 1.¹

153 As an instantiation of our framework, we use a mix of ADAM, which is popular in deep learning community, and
 154 an APPROXCUBICDESCENT for the practical reasons mentioned in Section 3.3. This method with ADAM and
 155 APPROXCUBICDESCENT. The parameters of these algorithms were chosen to produce the best generalization
 156 on a held out test set. The regularization parameter M was chosen as the smallest value such that the function
 157 value does not fluctuate in the first 10 epochs. We use the initialization suggested in [20] and a mini-batch size
 158 of 1000 for all the algorithms. We report objective function value against wall clock time and ISO calls.

159 The results are presented in Figure 2, which shows that our proposed mix framework was the *fastest* to escape
 160 the saddle point in terms of wall clock time. ADAM took considerably more time to escape the saddle point,
 161 especially in the case of MNIST. While APPROXCUBICDESCENT escaped the saddle point in relatively fewer
 162 iterations, each iteration required considerably large number of ISO calls; as a result, the method was extremely
 163 slow in terms of wall clock time, despite our efforts to improve it via approximations and code optimizations.
 164 On the other hand, our proposed framework, seamlessly balances these two methods, thereby, resulting in the
 165 fast decrease of training loss.

¹Data available at: www.cs.toronto.edu/~jmartens/digs3pts_1.mat,mnist_all.mat

References

- 166 [1] Alekh Agarwal and Leon Bottou. A lower bound for the optimization of finite sums. *arXiv:1410.0723*,
167 2014.
168
- 169 [2] Naman Agarwal, Zeyuan Allen Zhu, Brian Bullins, Elad Hazan, and Tengyu Ma. Finding approximate
170 local minima for nonconvex optimization in linear time. *CoRR*, abs/1611.01146, 2016.
- 171 [3] Léon Bottou. Stochastic gradient learning in neural networks. *Proceedings of Neuro-Nimes*, 91(8), 1991.
- 172 [4] Yair Carmon, John C. Duchi, Oliver Hinder, and Aaron Sidford. Accelerated methods for non-convex
173 optimization. *CoRR*, abs/1611.00756, 2016.
- 174 [5] C. Cartis and K. Scheinberg. Global convergence rate analysis of unconstrained optimization methods
175 based on probabilistic models. *Mathematical Programming*, pages 1–39, 2017. ISSN 1436-4646. doi:
176 10.1007/s10107-017-1137-4.
- 177 [6] Aaron Defazio, Francis Bach, and Simon Lacoste-Julien. SAGA: A fast incremental gradient method
178 with support for non-strongly convex composite objectives. In *NIPS 27*, pages 1646–1654, 2014.
- 179 [7] Aaron J Defazio, Tibério S Caetano, and Justin Domke. Finito: A faster, permutable incremental gradient
180 method for big data problems. *arXiv:1407.2710*, 2014.
- 181 [8] Rong Ge, Furong Huang, Chi Jin, and Yang Yuan. Escaping from saddle points - online stochastic
182 gradient for tensor decomposition. In *Proceedings of The 28th Conference on Learning Theory, COLT*
183 *2015*, pages 797–842, 2015.
- 184 [9] Saeed Ghadimi and Guanghai Lan. Stochastic first- and zeroth-order methods for nonconvex stochastic
185 programming. *SIAM Journal on Optimization*, 23(4):2341–2368, 2013. doi: 10.1137/120880811.
- 186 [10] Geoffrey E Hinton and Ruslan R Salakhutdinov. Reducing the dimensionality of data with neural
187 networks. *science*, 313(5786):504–507, 2006.
- 188 [11] Chi Jin, Rong Ge, Praneeth Netrapalli, Sham M. Kakade, and Michael I. Jordan. How to escape saddle
189 points efficiently. *CoRR*, abs/1703.00887, 2017.
- 190 [12] Rie Johnson and Tong Zhang. Accelerating stochastic gradient descent using predictive variance reduction.
191 In *NIPS 26*, pages 315–323, 2013.
- 192 [13] Diederik P. Kingma and Jimmy Ba. Adam: A method for stochastic optimization. *CoRR*, abs/1412.6980,
193 2014.
- 194 [14] Jakub Konečný, Jie Liu, Peter Richtárik, and Martin Takáč. Mini-Batch Semi-Stochastic Gradient
195 Descent in the Proximal Setting. *arXiv:1504.04407*, 2015.
- 196 [15] Harold Joseph Kushner and Dean S Clark. *Stochastic approximation methods for constrained and*
197 *unconstrained systems*, volume 26. Springer Science & Business Media, 2012.
- 198 [16] Guanghai Lan and Yi Zhou. An optimal randomized incremental gradient method. *arXiv:1507.02000*,
199 2015.
- 200 [17] Kfir Y. Levy. The power of normalization: Faster evasion of saddle points. *CoRR*, abs/1611.04831, 2016.
- 201 [18] Xiangru Lian, Yijun Huang, Yuncheng Li, and Ji Liu. Asynchronous Parallel Stochastic Gradient for
202 Nonconvex Optimization. In *NIPS*, 2015.
- 203 [19] Lennart Ljung. Analysis of recursive stochastic algorithms. *Automatic Control, IEEE Transactions on*,
204 22(4):551–575, 1977.
- 205 [20] James Martens. Deep learning via hessian-free optimization. In *Proceedings of the 27th International*
206 *Conference on Machine Learning (ICML-10)*, pages 735–742, 2010.
- 207 [21] James Martens and Roger Grosse. Optimizing neural networks with kronecker-factored approximate
208 curvature. In *International Conference on Machine Learning*, pages 2408–2417, 2015.
- 209 [22] Yurii Nesterov. *Introductory Lectures On Convex Optimization: A Basic Course*. Springer, 2003.
- 210 [23] Yurii Nesterov and Boris T Polyak. Cubic regularization of newton method and its global performance.
211 *Mathematical Programming*, 108(1):177–205, 2006.

- 212 [24] BT Poljak and Ya Z Tsypkin. Pseudogradient adaptation and training algorithms. *Automation and*
213 *Remote Control*, 34:45–67, 1973.
- 214 [25] Sashank Reddi, Ahmed Hefny, Suvrit Sra, Barnabas Poczos, and Alex J Smola. On variance reduction in
215 stochastic gradient descent and its asynchronous variants. In *NIPS 28*, pages 2629–2637, 2015.
- 216 [26] Sashank J. Reddi, Ahmed Hefny, Suvrit Sra, Barnabás Póczos, and Alexander J. Smola. Stochastic
217 variance reduction for nonconvex optimization. In *Proceedings of the 33rd International Conference on*
218 *Machine Learning, ICML 2016, New York City, NY, USA, June 19-24, 2016*, pages 314–323, 2016.
- 219 [27] Sashank J. Reddi, Suvrit Sra, Barnabás Póczos, and Alexander J. Smola. Fast incremental method for
220 nonconvex optimization. *CoRR*, abs/1603.06159, 2016.
- 221 [28] Sashank J. Reddi, Suvrit Sra, Barnabás Póczos, and Alexander J. Smola. Fast stochastic methods for
222 nonsmooth nonconvex optimization. *CoRR*, 2016.
- 223 [29] H. Robbins and S. Monro. A stochastic approximation method. *Annals of Mathematical Statistics*, 22:
224 400–407, 1951.
- 225 [30] Mark W. Schmidt, Nicolas Le Roux, and Francis R. Bach. Minimizing Finite Sums with the Stochastic
226 Average Gradient. *arXiv:1309.2388*, 2013.
- 227 [31] Shai Shalev-Shwartz and Tong Zhang. Stochastic dual coordinate ascent methods for regularized loss.
228 *The Journal of Machine Learning Research*, 14(1):567–599, 2013.
- 229 [32] Ilya Sutskever, James Martens, George Dahl, and Geoffrey Hinton. On the importance of initialization
230 and momentum in deep learning. In *International conference on machine learning*, pages 1139–1147,
231 2013.
- 232 [33] Oriol Vinyals and Daniel Povey. Krylov subspace descent for deep learning. In *AISTATS*, pages
233 1261–1268, 2012.

Appendix: A Generic Approach for Escaping Saddle points

235 A Related Works

236 There is a vast literature on algorithms for solving optimization problems of the form (1). A classical approach
 237 for solving such optimization problems is SGD, which dates back at least to the seminal work of [29]. Since
 238 then, SGD has been a subject of extensive research, especially in the convex setting [3, 15, 19, 24]. Recently,
 239 new faster methods, called variance reduced (VR) methods, have been proposed for convex finite-sum
 240 problems. VR methods attain faster convergence by reducing the variance in the stochastic updates of SGD, see
 241 e.g., [6, 7, 12, 14, 30, 31]. Accelerated variants of these methods achieve the lower bounds proved in [1, 16],
 242 thereby settling the question of their optimality. Furthermore, [25] developed an asynchronous framework for
 243 VR methods and demonstrated their benefits in parallel environments.

244 Most of the aforementioned prior works study stochastic methods in convex or very specialized nonconvex
 245 settings that admit theoretical guarantees on sub-optimality. For the general nonconvex setting, it is only
 246 recently that non-asymptotic convergence rate analysis for SGD and its variants was obtained in [9], who
 247 showed that SGD ensures $\|\nabla f\| \leq \epsilon$ (in expectation) in $O(1/\epsilon^4)$ iterations. A similar rate for parallel and
 248 distributed SGD was shown in [18]. For these problems, Reddi et al. [26, 27, 28] proved faster convergence
 249 rates that ensure the same optimality criteria in $O(n + n^{2/3}/\epsilon^2)$, which is an order $n^{1/3}$ faster than GD. While
 250 these methods ensure convergence to *stationary* points at a faster rate, the question of convergence to local
 251 minima (or in general to second-order critical points) has not been addressed. To our knowledge, convergence
 252 rates to second-order critical points (defined in Definition 1) for general nonconvex functions was first studied
 253 by [23]. However, each iteration of the algorithm in [23] is prohibitively expensive since it requires eigenvalue
 254 decompositions, and hence, is unsuitable for large-scale high-dimensional problems. More recently, Agarwal
 255 et al. [2], Carmon et al. [4] presented algorithms for finding second-order critical points by tackling some
 256 practical issues that arise in [23]. However, these algorithms are either only applicable to a restricted setting or
 257 heavily use Hessian based computations, making them unappealing from a practical standpoint. *Noisy* variants
 258 of first-order methods have also been shown to escape saddle points (see [8, 11, 17]), however, these methods
 259 have strong dependence on either n or d , both of which are undesirable.

260 B Proof of Theorem 1

261 The case of $\tau = \emptyset$ can be handled in a straightforward manner, so let us focus on the case where $\tau = \diamond$. We
 262 split our analysis into cases, each analyzing the change in objective function value depending on second-order
 263 criticality of y^t .

264 We start with the case where the gradient condition of second-order critical point is violated and then proceed
 265 to the case where the Hessian condition is violated.

266 **Case I:** $\mathbb{E}[\|\nabla f(y^t)\|] \geq \epsilon$ for some $t > 0$

267 We first observe the following: $\mathbb{E}[\|\nabla f(y^t)\|^2] \geq (\mathbb{E}\|\nabla f(y^t)\|)^2 \geq \epsilon^2$. This follows from a straightforward
 268 application of Jensen's inequality. From this inequality, we have the following:

$$\epsilon^2 \leq \mathbb{E}[\|\nabla f(y^t)\|^2] \leq \frac{1}{g(n, \epsilon)} \mathbb{E}[f(x^{t-1}) - f(z^t)]. \quad (2)$$

This follows from the fact that y^t is the output of GRADIENT-FOCUSED-OPTIMIZER subroutine, which
 satisfies the condition that for $(y, z) = \text{GRADIENT-FOCUSED-OPTIMIZER}(x, n, \epsilon)$, we have

$$\mathbb{E}[\|\nabla f(y)\|^2] \leq \frac{1}{g(n, \epsilon)} \mathbb{E}[f(x) - f(z)].$$

From Equation (2), we have

$$\mathbb{E}[f(z^t)] \leq \mathbb{E}[f(x^{t-1})] - \epsilon^2 g(n, \epsilon).$$

269 Furthermore, due to the property of non-increasing nature of GRADIENT-FOCUSED-OPTIMIZER, we also
 270 have $\mathbb{E}[y^t] \leq \mathbb{E}[f(x^{t-1})]$.

271 We now focus on the HESSIAN-FOCUSED-OPTIMIZER subroutine. From the property of
 272 HESSIAN-FOCUSED-OPTIMIZER that the objective function value is non-increasing, we have

273 $\mathbb{E}[f(x^t)] \leq \mathbb{E}[f(u^t)]$. Therefore, combining with the above inequality, we have

$$\begin{aligned}
\mathbb{E}[f(x^t)] &\leq \mathbb{E}[f(u^t)] \\
&= p\mathbb{E}[f(y^t)] + (1-p)\mathbb{E}[f(z^t)] \\
&\leq p\mathbb{E}[f(x^{t-1})] + (1-p)(\mathbb{E}[f(x^{t-1})] - \epsilon^2 g(n, \epsilon)) \\
&= \mathbb{E}[f(x^{t-1})] - (1-p)\epsilon^2 g(n, \epsilon).
\end{aligned} \tag{3}$$

274 The first equality is due to the definition of u^t in Algorithm 1. Therefore, when the gradient condition is
275 violated, irrespective of whether $\lambda_{\min}(\nabla^2 f(x)) \leq -\gamma$ or $\nabla^2 f(y^t) \succeq -\gamma\mathbb{I}$, the objective function value always
276 decreases by at least $\epsilon^2 g(n, \epsilon)$.

277 **Case II:** $\mathbb{E}[\|\nabla f(y^t)\|] < \epsilon$ and $\lambda_{\min}(\nabla^2 f(x)) \leq -\gamma$ for some $t > 0$

In this case, we first note that for $y = \text{HESSIAN-FOCUSED-OPTIMIZER}(x, n, \epsilon, \gamma)$ and $\lambda_{\min}(\nabla^2 f(x)) \leq -\gamma$,
we have $\mathbb{E}[f(y)] \leq f(x) - h(n, \epsilon, \gamma)$. Observe that $x^t = \text{HESSIAN-FOCUSED-OPTIMIZER}(u^t, n, \epsilon, \gamma)$.
Therefore, if $u^t = y^t$ and $\lambda_{\min}(\nabla^2 f(x)) \leq -\gamma$, then we have

$$\mathbb{E}[f(x^t)|u^t = y^t] \leq f(y^t) - h(n, \epsilon, \gamma) \leq f(x^{t-1}) - h(n, \epsilon, \gamma).$$

278 The second inequality is due to the non-increasing property of GRADIENT-FOCUSED-OPTIMIZER. On the
279 other hand, if $u^t = z^t$, we have hand, if we have $\mathbb{E}[f(x^t)|u^t = z^t] \leq f(z^t)$. This is due to the non-increasing
280 property of HESSIAN-FOCUSED-OPTIMIZER. Combining the above two inequalities and using the law of
281 total expectation, we get

$$\begin{aligned}
\mathbb{E}[f(x^t)] &= p\mathbb{E}[f(x^t)|u^t = y^t] + (1-p)\mathbb{E}[f(x^t)|u^t = z^t] \\
&\leq p(\mathbb{E}[f(y^t)] - h(n, \epsilon, \gamma)) + (1-p)\mathbb{E}[f(z^t)] \\
&\leq p(\mathbb{E}[f(x^{t-1})] - h(n, \epsilon, \gamma)) + (1-p)\mathbb{E}[f(x^{t-1})] \\
&= \mathbb{E}[f(x^{t-1})] - ph(n, \epsilon, \gamma).
\end{aligned} \tag{4}$$

282 The second inequality is due to the non-increasing property of GRADIENT-FOCUSED-OPTIMIZER. Therefore,
283 when the hessian condition is violated, the objective function value always decreases by at least $ph(n, \epsilon, \gamma)$.

284 **Case III:** $\mathbb{E}[\|\nabla f(y^t)\|] < \epsilon$ and $\nabla^2 f(y^t) \succeq -\gamma\mathbb{I}$ for some $t > 0$

285 This is the favorable case for the algorithm. The only condition to note is that the objective function value
286 will be non-increasing in this case too. This is, again, due to the non-increasing properties of subroutines
287 GRADIENT-FOCUSED-OPTIMIZER and HESSIAN-FOCUSED-OPTIMIZER. In general, greater the occurrence
288 of this case during the course of the algorithm, higher will the probability that the output of our algorithm
289 satisfies the desired property.

The key observation is that Case I & II cannot occur large number of times since each of these cases strictly
decreases the objective function value. In particular, from Equation (3) and (4), it is easy to see that each
occurrence of Case I & II the following holds:

$$\mathbb{E}[f(x^t)] \leq \mathbb{E}[f(x^{t-1})] - \theta,$$

290 where $\theta = \min((1-p)\epsilon^2 g(n, \epsilon), ph(n, \epsilon, \gamma))$. Furthermore, the function f is lower bounded by B , thus, Case
291 I & II cannot occur more than $(f(x^0) - B)/\theta$ times. Therefore, the probability of occurrence of Case III is at
292 least $1 - (f(x^0) - B)/(T\theta)$, which completes the first part of the proof.

293 The second part of the proof simply follows from first part. As seen above, the probability of Case I & II
294 is at most $(f(x^0) - B)/T\theta$. Therefore, probability that an element of the set S falls in Case III is at least
295 $1 - ((f(x^0) - B)/T\theta)^k$, which gives us the required result for the second part.

296 C SVRG and Proof of Lemma 1

297 SVRG [12, 26] is a stochastic algorithm recently shown to be very effective for reducing variance in finite-sum
298 problems. We seek to understand its benefits for nonconvex optimization, with a particular focus on the issue
299 of escaping saddle points. Algorithm 2 presents SVRG's pseudocode.

300 Observe that Algorithm 2 is an epoch-based algorithm. At the start of each epoch s , a full gradient is calculated
301 at the point \tilde{x}^s , requiring n calls to the IFO. Within its inner loop SVRG performs m stochastic updates.
302 Suppose m is chosen to be $O(n)$ (typically used in practice), then the total IFO calls per epoch is $\Theta(n)$. Strong
303 convergence rates have been proved Algorithm 2 in the context of convex and nonconvex optimization [12, 26]

Algorithm 2 SVRG(x^0, ϵ)

1: **Input:** $x_m^0 = x^0 \in \mathbb{R}^d$, epoch length m , step sizes $\{\eta_i > 0\}_{i=0}^{m-1}$, iterations $T_g, S = \lceil T_g/m \rceil$
2: **for** $s = 0$ **to** $S - 1$ **do**
3: $\tilde{x}^s = x_0^{s+1} = x_m^s$
4: $g^{s+1} = \frac{1}{n} \sum_{i=1}^n \nabla f_i(\tilde{x}^s)$
5: **for** $t = 0$ **to** $m - 1$ **do**
6: Uniformly randomly pick i_t from $\{1, \dots, n\}$
7: $v_t^{s+1} = \nabla f_{i_t}(x_t^{s+1}) - \nabla f_{i_t}(\tilde{x}^s) + g^{s+1}$
8: $x_{t+1}^{s+1} = x_t^{s+1} - \eta_t v_t^{s+1}$
9: **end for**
10: **end for**
11: **Output:** (y, z) where y is Iterate x_a chosen uniformly random from $\{\{x_t^{s+1}\}_{t=0}^{m-1}\}_{s=0}^{S-1}$ and $z = x_m^S$.

304 *Proof of Lemma 1.* The proof follows from the analysis in [26] with some additional reasoning. We need to
305 show two properties: **G.1** and **G.2**, both of which are based on objective function value. To this end, we start
306 with an update in the s^{th} epoch. We have the following:

$$\begin{aligned} \mathbb{E}[f(x_{t+1}^{s+1})] &\leq \mathbb{E}[f(x_t^{s+1}) + \langle \nabla f(x_t^{s+1}), x_{t+1}^{s+1} - x_t^{s+1} \rangle + \frac{L}{2} \|x_{t+1}^{s+1} - x_t^{s+1}\|^2] \\ &\leq \mathbb{E}[f(x_t^{s+1}) - \eta_t \|\nabla f(x_t^{s+1})\|^2 + \frac{L\eta_t^2}{2} \|v_t^{s+1}\|^2]. \end{aligned} \quad (5)$$

The first inequality is due to L -smoothness of the function f . The second inequality simply follows from the unbiasedness of SVRG update in Algorithm 2. For the analysis of the algorithm, we need the following Lyapunov function:

$$A_t^{s+1} := \mathbb{E}[f(x_t^{s+1}) + \mu_t \|x_t^{s+1} - \tilde{x}^s\|^2].$$

This function is a combination of objective function and the distance of the current iterate from the latest snapshot \tilde{x}^s . Note that the term μ_t is introduced only for the analysis and is not part of the algorithm (see Algorithm 2). Here $\{\mu_t\}_{t=0}^m$ is chosen such the following holds:

$$\mu_t = \mu_{t+1}(1 + \eta_t \beta_t + 2\eta_t^2 L^2) + \eta_t^2 L^3,$$

307 for all $t \in \{0, \dots, m-1\}$ and $\mu_m = 0$. For bounding the Lyapunov function A , we need the following bound
308 on the distance of the current iterate from the latest snapshot:

$$\begin{aligned} \mathbb{E}[\|x_{t+1}^{s+1} - \tilde{x}^s\|^2] &= \mathbb{E}[\|x_{t+1}^{s+1} - x_t^{s+1} + x_t^{s+1} - \tilde{x}^s\|^2] \\ &= \mathbb{E}[\|x_{t+1}^{s+1} - x_t^{s+1}\|^2 + \|x_t^{s+1} - \tilde{x}^s\|^2 + 2\langle x_{t+1}^{s+1} - x_t^{s+1}, x_t^{s+1} - \tilde{x}^s \rangle] \\ &= \mathbb{E}[\eta_t^2 \|v_t^{s+1}\|^2 + \|x_t^{s+1} - \tilde{x}^s\|^2 - 2\eta_t \mathbb{E}[\langle \nabla f(x_t^{s+1}), x_t^{s+1} - \tilde{x}^s \rangle]] \\ &\leq \mathbb{E}[\eta_t^2 \|v_t^{s+1}\|^2 + \|x_t^{s+1} - \tilde{x}^s\|^2] + 2\eta_t \mathbb{E}\left[\frac{1}{2\beta_t} \|\nabla f(x_t^{s+1})\|^2 + \frac{1}{2}\beta_t \|x_t^{s+1} - \tilde{x}^s\|^2\right]. \end{aligned} \quad (6)$$

309 The second equality is due to the unbiasedness of the update of SVRG. The last inequality follows from a
310 simple application of Cauchy-Schwarz and Young's inequality. Substituting Equation (5) and Equation (6)
311 into the Lyapunov function A_{t+1}^{s+1} , we obtain the following:

$$\begin{aligned} A_{t+1}^{s+1} &\leq \mathbb{E}[f(x_t^{s+1}) - \eta_t \|\nabla f(x_t^{s+1})\|^2 + \frac{L\eta_t^2}{2} \|v_t^{s+1}\|^2] \\ &\quad + \mathbb{E}[\mu_{t+1} \eta_t^2 \|v_t^{s+1}\|^2 + \mu_{t+1} \|x_t^{s+1} - \tilde{x}^s\|^2] \\ &\quad + 2\mu_{t+1} \eta_t \mathbb{E}\left[\frac{1}{2\beta_t} \|\nabla f(x_t^{s+1})\|^2 + \frac{1}{2}\beta_t \|x_t^{s+1} - \tilde{x}^s\|^2\right] \\ &\leq \mathbb{E}[f(x_t^{s+1}) - \left(\eta_t - \frac{\mu_{t+1}\eta_t}{\beta_t}\right) \|\nabla f(x_t^{s+1})\|^2] \\ &\quad + \left(\frac{L\eta_t^2}{2} + \mu_{t+1}\eta_t^2\right) \mathbb{E}[\|v_t^{s+1}\|^2] + (\mu_{t+1} + \mu_{t+1}\eta_t\beta_t) \mathbb{E}[\|x_t^{s+1} - \tilde{x}^s\|^2]. \end{aligned} \quad (7)$$

312 To further bound this quantity, we use Lemma 3 to bound $\mathbb{E}[\|v_t^{s+1}\|^2]$, so that upon substituting it in Equa-
313 tion (7), we see that

$$\begin{aligned} A_{t+1}^{s+1} &\leq \mathbb{E}[f(x_t^{s+1})] - \left(\eta_t - \frac{\mu_{t+1}\eta_t}{\beta_t} - \eta_t^2 L - 2\mu_{t+1}\eta_t^2\right) \mathbb{E}[\|\nabla f(x_t^{s+1})\|^2] \\ &\quad + [\mu_{t+1}(1 + \eta_t\beta_t + 2\eta_t^2 L^2) + \eta_t^2 L^3] \mathbb{E}[\|x_t^{s+1} - \tilde{x}^s\|^2] \\ &\leq A_t^{s+1} - \left(\eta_t - \frac{\mu_{t+1}\eta_t}{\beta_t} - \eta_t^2 L - 2\mu_{t+1}\eta_t^2\right) \mathbb{E}[\|\nabla f(x_t^{s+1})\|^2]. \end{aligned}$$

314 The second inequality follows from the definition of μ_t and A_t^{s+1} . Since $\eta_t = \eta = 1/(4Ln^{2/3})$ for $j > 0$ and
 315 $t \in \{0, \dots, j-1\}$,

$$A_j^{s+1} \leq A_0^{s+1} - v_n \sum_{t=0}^{j-1} \mathbb{E}[\|\nabla f(x_t^{s+1})\|^2], \quad (8)$$

where

$$v_n = \left(\eta_t - \frac{\mu_{t+1}\eta_t}{\beta_t} - \eta_t^2 L - 2\mu_{t+1}\eta_t^2\right).$$

We will prove that for the given parameter setting $v_n > 0$ (see the proof below). With $v_n > 0$, it is easy to see that $A_j^{s+1} \leq A_0^{s+1}$. Furthermore, note that $A_0^{s+1} = \mathbb{E}[f(x_0^{s+1}) + \mu_0\|x_0^{s+1} - \tilde{x}^s\|^2] = \mathbb{E}[f(x_0^{s+1})]$ since $x_0^{s+1} = \tilde{x}^s$ (see Algorithm 2). Also, we have

$$\mathbb{E}[f(x_j^{s+1}) + \mu_j\|x_j^{s+1} - \tilde{x}^s\|^2] \leq \mathbb{E}[f(x_0^{s+1})]$$

316 and thus, we obtain $\mathbb{E}[f(x_j^{s+1})] \leq \mathbb{E}[f(x_0^{s+1})]$ for all $j \in \{0, \dots, m\}$. Furthermore, using simple induction
 317 and the fact that $x_0^{s+1} = x_m^s$ for all epoch $s \in \{0, \dots, S-1\}$, it easy to see that $\mathbb{E}[f(x_j^{s+1})] \leq f(x^0)$.
 318 Therefore, with the definition of y specified in the output of Algorithm 2, we see that the condition **G.1** of
 319 GRADIENT-FOCUSED-OPTIMIZER is satisfied for SVRG algorithm.

320 We now prove that $v_n > 0$ and also **G.2** of GRADIENT-FOCUSED-OPTIMIZER is satisfied for SVRG algorithm.
 321 By using telescoping the sum with $j = m$ in Equation (8), we obtain

$$\sum_{t=0}^{m-1} \mathbb{E}[\|\nabla f(x_t^{s+1})\|^2] \leq \frac{A_0^{s+1} - A_m^{s+1}}{v_n}.$$

322 This inequality in turn implies that

$$\sum_{t=0}^{m-1} \mathbb{E}[\|\nabla f(x_t^{s+1})\|^2] \leq \frac{\mathbb{E}[f(\tilde{x}^s) - f(\tilde{x}^{s+1})]}{v_n}, \quad (9)$$

323 where we used that $A_m^{s+1} = \mathbb{E}[f(x_m^{s+1})] = \mathbb{E}[f(\tilde{x}^{s+1})]$ (since $\mu_m = 0$), and that $A_0^{s+1} = \mathbb{E}[f(\tilde{x}^s)]$ (since
 324 $x_0^{s+1} = \tilde{x}^s$). Now sum over all epochs to obtain

$$\frac{1}{T_g} \sum_{s=0}^{S-1} \sum_{t=0}^{m-1} \mathbb{E}[\|\nabla f(x_t^{s+1})\|^2] \leq \frac{\mathbb{E}[f(x^0) - f(x_m^S)]}{T_g v_n}. \quad (10)$$

325 Here we used the the fact that $\tilde{x}^0 = x^0$. To obtain a handle on v_n and complete our analysis, we will require
 326 an upper bound on μ_0 . We observe that $\mu_0 = \frac{L}{16n^{4/3}} \frac{(1+\theta)^{m-1}}{\theta}$ where $\theta = 2\eta^2 L^2 + \eta\beta$. This is obtained using
 327 the relation $\mu_t = \mu_{t+1}(1 + \eta\beta + 2\eta^2 L^2) + \eta^2 L^3$ and the fact that $\mu_m = 0$. Using the specified values of β
 328 and η we have

$$\theta = 2\eta^2 L^2 + \eta\beta = \frac{1}{8n^{4/3}} + \frac{1}{4n} \leq \frac{3}{4n}.$$

329 Using the above bound on θ , we get

$$\begin{aligned} \mu_0 &= \frac{L}{16n^{4/3}} \frac{(1+\theta)^m - 1}{\theta} = \frac{L((1+\theta)^m - 1)}{2(1+2n^{1/3})} \\ &\leq \frac{L((1+\frac{3}{4n})^{4n/3} - 1)}{2(1+2n^{1/3})} \leq n^{-1/3}(L(e-1)/4), \end{aligned} \quad (11)$$

330 wherein the second inequality follows upon noting that $(1+\frac{1}{l})^l$ is increasing for $l > 0$ and $\lim_{l \rightarrow \infty} (1+\frac{1}{l})^l = e$
 331 (here e is the Euler's number). Now we can lower bound v_n , as

$$v_n = \min_t \left(\eta - \frac{\mu_{t+1}\eta}{\beta} - \eta^2 L - 2\mu_{t+1}\eta^2\right) \geq \left(\eta - \frac{\mu_0\eta}{\beta} - \eta^2 L - 2\mu_0\eta^2\right) \geq \frac{1}{40Ln^{2/3}}.$$

332 The first inequality holds since μ_t decreases with t . The second inequality holds since (a) μ_0/β can be upper
 333 bounded by $(e-1)/4$ (follows from Equation (11)), (b) $\eta^2 L \leq \eta/4$ and (c) $2\mu_0\eta^2 \leq (e-1)\eta/8$ (follows
 334 from Equation (11)). Substituting the above lower bound in Equation (10), we obtain the following:

$$\frac{1}{T_g} \sum_{s=0}^{S-1} \sum_{t=0}^{m-1} \mathbb{E}[\|\nabla f(x_t^{s+1})\|^2] \leq \frac{40Ln^{2/3}\mathbb{E}[f(x^0) - f(x_m^S)]}{T_g}. \quad (12)$$

335 From the definition of (y, z) in output of Algorithm 2 i.e., y is Iterate x_a chosen uniformly random
 336 from $\{\{x_t^{s+1}\}_{t=0}^{m-1}\}_{s=0}^{S-1}$ and $z = x_m^S$, it is clear that Algorithm 2 satisfies the **G.2** requirement of
 337 GRADIENT-FOCUSED-OPTIMIZER with $g(n, \epsilon) = T_g/40Ln^{2/3}$. Since both **G.1** and **G.2** are satisfied
 338 for Algorithm 2, we conclude that SVRG is a GRADIENT-FOCUSED-OPTIMIZER. \square

Algorithm 3 HESSIANDESCENT (x, ϵ, γ)

- 1: Find v such that $\|v\| = 1$, and with probability at least ρ the following inequality holds: $\langle v, \nabla^2 f(x)v \rangle \leq \lambda_{\min}(\nabla^2 f(x)) + \frac{\gamma}{2}$.
 - 2: Set $\alpha = |\langle v, \nabla^2 f(x)v \rangle|/M$.
 - 3: $u = x - \alpha \text{sign}(\langle v, \nabla^2 f(x)v \rangle)v$.
 - 4: $y = \arg \min_{z \in \{u, x\}} f(z)$
 - 5: **Output:** (y, \diamond) .
-

339 D Hessian Descent and Proof of Lemma 2

340 The approach is based on directly using the eigenvector corresponding to the smallest eigenvalue as a
341 HESSIAN-FOCUSED-OPTIMIZER. More specifically, when the smallest eigenvalue of the Hessian is negative
342 and reasonably large in magnitude, the Hessian information can be used to ensure descent in the objective
343 function value. The pseudo-code for the algorithm is given in Algorithm 3.

344 The key idea is to utilize the minimum eigenvalue information in order to make a descent step. If
345 $\lambda_{\min}(\nabla^2 f(x)) \leq -\gamma$ then the idea is to use this information to take a descent step. Note the subroutine is
346 designed in a fashion such that the objective function value never increases. Thus, it naturally satisfies the
347 requirement **H.1** of HESSIAN-FOCUSED-OPTIMIZER.

348 **Proposition 1.** *The time complexity of finding $v \in \mathbb{R}^d$ that $\|v\| = 1$, and with probability at least ρ the*
349 *following inequality holds: $\langle v, \nabla^2 f(x)v \rangle \leq \lambda_{\min}(\nabla^2 f(x)) + \frac{\gamma}{2}$ is $O(nd + n^{3/4}d/\gamma^{1/2})$.*

350 Note that each iteration of Algorithm 1 in this case has just linear dependence on d . Since the total num-
351 ber of HESSIANDESCENT iterations is $O(\Delta/\min(p, 1-p)\epsilon^{3/2})$ and each iteration has the complexity of
352 $O(nd + n^{3/4}d/\epsilon^{1/4})$, using the above remark, we obtain an overall time complexity of HESSIANDESCENT is
353 $O(nd/\epsilon^{3/2} + n^{3/4}d/\epsilon^{7/4})$.

Proof of Lemma 2. The first important observation is that the function value never increases because $y =$
 $\arg \min_{z \in \{u, x\}} f(z)$ i.e., $f(y) \leq f(x)$, thus satisfying **H.1** of HESSIAN-FOCUSED-OPTIMIZER. We now
analyze the scenario where $\lambda_{\min}(\nabla^2 f(x)) \leq -\gamma$. Consider the event where we obtain v such that

$$\langle v, \nabla^2 f(x)v \rangle \leq \lambda_{\min}(\nabla^2 f(x)) + \frac{\gamma}{2}.$$

354 This event (denoted by \mathcal{E}) happens with at least probability ρ . Note that, since $\lambda_{\min}(\nabla^2 f(x)) \leq -\gamma$, we have
355 $\langle v, \nabla^2 f(x)v \rangle \leq -\frac{\gamma}{2}$. In this case, we have the following relationship:

$$\begin{aligned} f(y) &\leq f(x) + \langle \nabla f(x), y - x \rangle + \frac{1}{2}(y - x)^T \nabla^2 f(x)(y - x) + \frac{M}{6} \|y - x\|^3 \\ &= f(x) - \alpha |\langle \nabla f(x), v \rangle| + \frac{\alpha^2}{2} v^T \nabla^2 f(x)v + \frac{M\alpha^3}{6} \|v\|^3 \\ &\leq f(x) + \frac{\alpha^2}{2} v^T \nabla^2 f(x)v + \frac{M\alpha^3}{6} \\ &\leq f(x) - \frac{1}{2M^2} |v^T \nabla^2 f(x)v|^3 + \frac{1}{6M^2} |v^T \nabla^2 f(x)v|^3 \\ &= f(x) - \frac{1}{3M^2} |v^T \nabla^2 f(x)v|^3 \leq f(x) - \frac{1}{24M^2} \gamma^3. \end{aligned} \tag{13}$$

The first inequality follows from the M -lipschitz continuity of the Hessian $\nabla^2 f(x)$. The first equality follows
from the update rule of HESSIANDESCENT. The second inequality is obtained by dropping the negative term
and using the fact that $\|v\| = 1$. The second equality is obtained by substituting $\alpha = \frac{|v^T \nabla^2 f(x)v|}{M}$. The last
inequality is due to the fact that $\langle v, \nabla^2 f(x)v \rangle \leq -\frac{\gamma}{2}$. In the other scenario where

$$\langle v, \nabla^2 f(x)v \rangle \leq \lambda_{\min}(\nabla^2 f(x)) + \frac{\gamma}{2},$$

356 we can at least ensure that $f(y) \leq f(x)$ since $y = \arg \min_{z \in \{u, x\}} f(z)$. Therefore, we have

$$\begin{aligned} \mathbb{E}[f(y)] &= \rho \mathbb{E}[f(y)|\mathcal{E}] + (1 - \rho) \mathbb{E}[f(y)|\mathcal{E}^c] \\ &\leq \rho \mathbb{E}[f(y)|\mathcal{E}] + (1 - \rho) f(x) \\ &\leq \rho \left[f(x) - \frac{\rho}{24M^2} \gamma^3 \right] + (1 - \rho) f(x) \\ &= f(x) - \frac{\rho}{24M^2} \gamma^3. \end{aligned} \tag{14}$$

357 The last inequality is due to Equation (13). Hence, HESSIAN-FOCUSED-OPTIMIZER satisfies **H.2** of
 358 HESSIAN-FOCUSED-OPTIMIZER with $h(n, \epsilon, \gamma) = \frac{\rho}{24M^2}\gamma^3$, thus concluding the proof. \square

359 E Other Lemmas

360 The following bound on the variance of SVRG is useful for our proof [26].

361 **Lemma 3.** [26] *Let v_t^{s+1} be computed by Algorithm 2. Then,*

$$\mathbb{E}[\|v_t^{s+1}\|^2] \leq 2\mathbb{E}[\|\nabla f(x_t^{s+1})\|^2] + 2L^2\mathbb{E}[\|x_t^{s+1} - \tilde{x}^s\|^2].$$

362 *Proof.* We use the definition of v_t^{s+1} to get

$$\begin{aligned} \mathbb{E}[\|v_t^{s+1}\|^2] &= \mathbb{E}[\|(\nabla f_{i_t}(x_t^{s+1}) - \nabla f_{i_t}(\tilde{x}^s)) + \nabla f(\tilde{x}^s)\|^2] \\ &= \mathbb{E}[\|(\nabla f_{i_t}(x_t^{s+1}) - \nabla f_{i_t}(\tilde{x}^s)) + \nabla f(\tilde{x}^s) - \nabla f(x_t^{s+1}) + \nabla f(x_t^{s+1})\|^2] \\ &\leq 2\mathbb{E}[\|\nabla f(x_t^{s+1})\|^2] + 2\mathbb{E}[\|\nabla f_{i_t}(x_t^{s+1}) - \nabla f_{i_t}(\tilde{x}^s) - \mathbb{E}[\nabla f_{i_t}(x_t^{s+1}) - \nabla f_{i_t}(\tilde{x}^s)]\|^2] \end{aligned}$$

363 The inequality follows from the simple fact that $(a + b)^2 \leq a^2 + b^2$. From the above inequality, we get the
 364 following:

$$\begin{aligned} \mathbb{E}[\|v_t^{s+1}\|^2] &\leq 2\mathbb{E}[\|\nabla f(x_t^{s+1})\|^2] + 2\mathbb{E}[\|\nabla f_{i_t}(x_t^{s+1}) - \nabla f_{i_t}(\tilde{x}^s)\|^2] \\ &\leq 2\mathbb{E}[\|\nabla f(x_t^{s+1})\|^2] + 2L^2\mathbb{E}[\|x_t^{s+1} - \tilde{x}^s\|^2] \end{aligned}$$

365 The first inequality follows by noting that for a random variable ζ , $\mathbb{E}[\|\zeta - \mathbb{E}[\zeta]\|^2] \leq \mathbb{E}[\|\zeta\|^2]$. The last
 366 inequality follows from L -smoothness of f_{i_t} . \square

367 F Cubic Regularization and its Approximation

368 In this section, we show that the cubic regularization method in [23] can be used as
 369 HESSIAN-FOCUSED-OPTIMIZER. More specifically, here HESSIAN-FOCUSED-OPTIMIZER approximately
 370 solves the following optimization problem:

$$y = \arg \min_z \langle \nabla f(x), z - x \rangle + \frac{1}{2} \langle z - x, \nabla^2 f(x)(z - x) \rangle + \frac{M}{6} \|z - x\|^3, \quad (\text{CUBICDESCENT})$$

371 and returns (y, \diamond) as output. The following result can be proved for this approach.

372 **Theorem 3.** *Suppose SVRG (same as Theorem 2) is used as GRADIENT-FOCUSED-OPTIMIZER and*
 373 *CUBICDESCENT is used as HESSIAN-FOCUSED-OPTIMIZER with $q = 0$, then Algorithm 1 finds a $(\epsilon, \sqrt{\epsilon})$ -*
 374 *second order critical point in $T = O(\Delta / \min(p, 1 - p)\epsilon^{3/2})$ with probability at least 0.9.*

375 *Proof.* First note that cubic method is a descent method (refer to Theorem 1 of [23]); thus, **H.1** is trivially
 376 satisfied. Furthermore, cubic descent is a HESSIAN-FOCUSED-OPTIMIZER with $h(n, \epsilon, \gamma) = \frac{2\gamma^3}{81M^3}\gamma^3$. This,
 377 again, follows from Theorem 1 of [23]. The result easily follows from the aforementioned observations. \square

378 In principle, Algorithm 1 with CUBICDESCENT as HESSIAN-FOCUSED-OPTIMIZER can converge without the
 379 use of GRADIENT-FOCUSED-OPTIMIZER subroutine at each iteration since it essentially reduces to the cubic
 380 regularization method of [23]. However, in practice, we would expect GRADIENT-FOCUSED-OPTIMIZER to
 381 perform most of the optimization and HESSIAN-FOCUSED-OPTIMIZER to be used for far fewer iterations.
 382 Using the method developed in [23] for solving CUBICDESCENT, we obtain the following corollary.

383 **Corollary 2.** *The overall running time of Algorithm 1 to find a $(\epsilon, \sqrt{\epsilon})$ -second order critical point, with*
 384 *parameter settings used in Theorem 3, is $O(nd^\omega / \epsilon^{3/2} + n^{2/3}d / \epsilon^2)$.*

385 Here ω is the matrix multiplication constant. The dependence on ϵ is weaker in comparison to Corollary 1.
 386 However, each iteration of CUBICDESCENT is expensive (as seen from the factor d^ω in the corollary above)
 387 and thus, in high dimensional settings typically encountered in machine learning, this approach can be
 388 expensive in comparison to HESSIANDESCENT.

389 Cubic regularization method of Nesterov and Polyak [23] is designed to operate on full batch, i.e., it does not
 390 exploit the finite-sum structure of the problem and requires the computation of the gradient and the Hessian
 391 on the entire dataset to make an update. However, such full-batch methods do not scale gracefully with the
 392 size of data and become prohibitively expensive on large datasets. To overcome this challenge, we devised an
 393 approximate cubic regularization method described below:

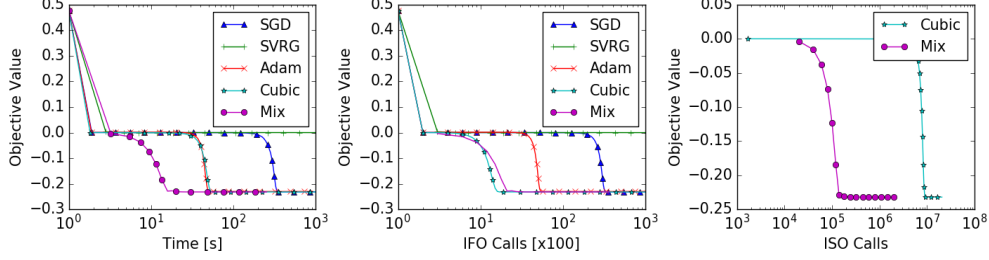


Figure 3: Comparison of various methods on a synthetic problem. Our mix framework successfully escapes saddle point and uses relatively few ISO calls in comparison to CUBICDESCENT.

394

1. Pick a mini-batch \mathcal{B} and obtain the gradient and the hessian based on \mathcal{B} , i.e.,

$$g = \frac{1}{|\mathcal{B}|} \sum_{i \in \mathcal{B}} \nabla f_i(x) \quad H = \frac{1}{|\mathcal{B}|} \sum_{i \in \mathcal{B}} \nabla^2 f_i(x) \quad (15)$$

395

2. Solve the sub-problem

$$v^* = \arg \min_v \langle g, v \rangle + \frac{1}{2} \langle v, H v \rangle + \frac{M}{6} \|v\|^3 \quad (16)$$

396

3. Update: $x \leftarrow x + v^*$

397

We found that this mini-batch training strategy, which requires the computation of the gradient and the Hessian on a small subset of the dataset, to work well on a few datasets (CURVES, MNIST, CIFAR10). A similar method has been analysed in [5].

400

Furthermore, in many deep-networks, adaptive per-parameter learning rate helps immensely [13]. One possible explanation for this is that the scale of the gradients in each layer of the network often differ by several orders of magnitude. A well-suited optimization method should take this into account. This is the reason for popularity of methods like ADAM or RMSPROP in the deep learning community. On similar lines, to account for different per-parameter behaviour in cubic regularization, we modify the sub-problem by adding a diagonal matrix M_d in addition to the scalar regularization coefficient M , i.e.,

402
403
404
405

$$\min_v \langle g, v \rangle + \frac{1}{2} \langle v, H v \rangle + \frac{1}{6} M \|M_d v\|^3. \quad (17)$$

406

Also we devised an adaptive rule to obtain the diagonal matrix as $M_d = \text{diag}((s + 10^{-12})^{1/9})$, where s is maintained as a moving average of third order polynomial of the mini-batch gradient g , in a fashion similar to RMSPROP and ADAM:

407
408

$$s \leftarrow \beta s + (1 - \beta)(|g|^3 + 2g^2), \quad (18)$$

409

where $|g|^3$ and g^2 are vectors such that $[|g|^3]_i = |g_i|^3$ and $[g^2]_i = g_i^2$ respectively for all $i \in [n]$. The experiments reported on CURVES and MNIST in this paper utilizes both the above modifications to the cubic regularization, with β set to 0.9. We refer to this modified procedure as ACubic in our results.

410
411

412 G Experiment Details

413

In this section we provide further experimental details and results to aid reproducibility.

414

Synthetic Problem To demonstrate the fast escape from a saddle point by the proposed method, we consider the following simple nonconvex finite-sum problem:

415

$$\min_{x \in \mathbb{R}^d} \frac{1}{n} \sum_{i=1}^n x^T A_i x + b_i^T x + \|x\|_{10}^{10} \quad (19)$$

416

Here the parameters are designed such that $\sum_i b_i = 0$ and $\sum_i A_i$ matrix has exactly one negative eigenvalue of -0.001 and other eigenvalues randomly chosen in the interval $[1, 2]$. The total number of examples n is set to be 100,000 and d is 1000. It is not hard to see that this problem has a non-degenerate saddle point at the origin. This allows us to explore the behaviour of different optimization algorithms in the vicinity of the saddle point. In this experiment, we compare a mix of SVRG and HESSIANDESCENT (as in Theorem 2) with SGD (with constant step size), ADAM, SVRG and CUBICDESCENT. The parameter of these algorithms is chosen by grid search so that it gives the best performance. The subproblem of CUBICDESCENT was solved with gradient descent [4] until the gradient norm of the subproblem is reduced below 10^{-3} . We study the progress

417

418

419

420

421

422

423

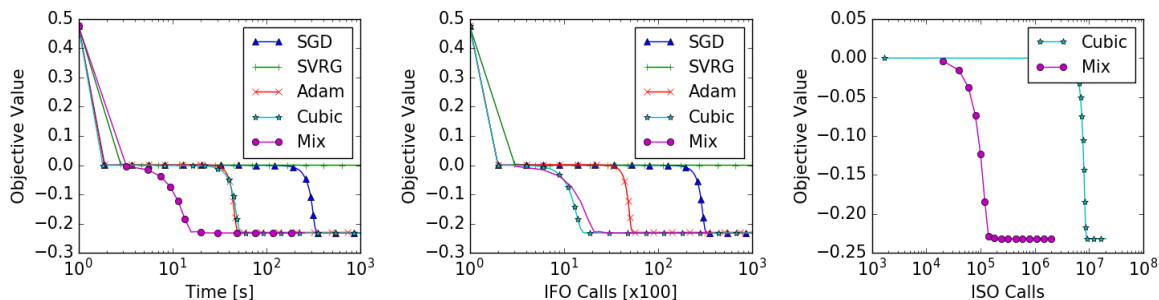


Figure 4: Comparison of various methods on a synthetic problem. Our mix framework successfully escapes saddle point.

424 of optimization, i.e., decrease in function value with wall clock time, IFO calls, and ISO calls. All algorithms
 425 were initialized with the same starting point very close to origin.

426 The results are presented in Figure 3, which shows that our proposed mix framework was the *fastest* to escape
 427 the saddle point in terms of wall clock time. We observe that performance of the first order methods suffered
 428 severely due to the saddle point. Note that SGD eventually escaped the saddle point due to inherent noise in
 429 the mini-batch gradient. CUBICDESCENT, a second-order method, escaped the saddle point faster in terms of
 430 iterations using the Hessian information. But operating on Hessian information is expensive as a result this
 431 method was slow in terms of wall clock time. The proposed framework, which is a mix of the two strategies,
 432 inherits the best of both worlds by using cheap gradient information most of the time and reducing the use of
 433 relatively expensive Hessian information (ISO calls) by 100x. This resulted in *faster* escape from saddle point
 434 in terms of wall clock time.

435 G.1 Synthetic Problem

436 The parameter selection for all the methods were carried as follows:

- 437 1. SGD: The scalar step-size was determined by a grid search.
- 438 2. ADAM: We performed a grid search over α and ε parameters of ADAM tied together, i.e., $\alpha = \varepsilon$.
- 439 3. SVRG: The scalar step-size was determined by a grid search.
- 440 4. CUBICDESCENT: The regularization parameter M was chosen by grid search. The sub-problem was solved
 441 with gradient descent [4] with the step-size of solver to be 10^{-2} and run till the gradient norm of the
 442 sub-problem is reduced below 10^{-3} .

443 **Further Observations** The results are presented in Figure 4. The other first order methods like ADAM with
 444 higher noise could escape relatively faster whereas SVRG with reduced noise stayed stuck at the saddle point.

445 G.2 Deep Networks

446 **Methods** The parameter selection for all the methods were carried as follows::

- 447 1. ADAM: We performed a grid search over α and ε parameters of ADAM so as to produce the best generaliza-
 448 tion on a held out test set. We found it to be $\alpha = 10^{-3}$, $\varepsilon = 10^{-3}$ for CURVES and $\alpha = 10^{-2}$, $\varepsilon = 10^{-1}$
 449 for MNIST.
- 450 2. APPROXCUBICDESCENT: The regularization parameter M was chosen as the largest value such function
 451 value does not jump in first 10 epochs. We found it to be $M = 10^3$ for both CURVES and MNIST. The
 452 sub-problem was solved with gradient descent [4] with the step-size of solver to be 10^{-3} and run till the
 453 gradient norm of the sub-problem is reduced below 0.1.

454 H Discussion

455 In this paper, we examined a generic strategy to escape saddle points in nonconvex finite-sum problems and
 456 presented its convergence analysis. The key intuition is to alternate between a first-order and second-order
 457 based optimizers; the latter is mainly intended to escape points that are only stationary but are not second-
 458 order critical points. We presented two different instantiations of our framework and provided their detailed
 459 convergence analysis. While both our methods explicitly use the Hessian information, one can also use noisy
 460 first-order methods as HESSIAN-FOCUSED-OPTIMIZER (see for e.g. noisy SGD in [8]). In such a scenario,
 461 we exploit the negative eigenvalues of the Hessian to escape saddle points by using isotropic noise, and do
 462 not explicitly use ISO. For these methods, under strict-saddle point property [8], we can show convergence to
 463 local optima within our framework.

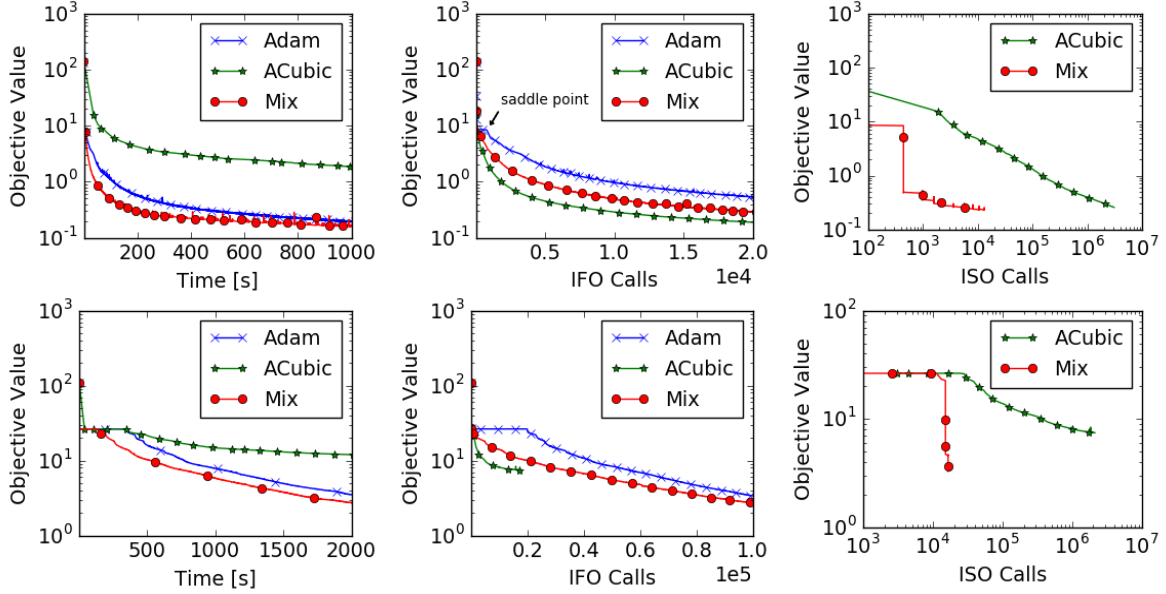


Figure 5: Comparison of various methods on a Deep Autoencoder on CURVES (top) and MNIST (bottom). Our mix approach converges faster than the baseline methods and uses relatively few ISO calls in comparison to APPROXCUBICDESCENT

464 We primarily focused on obtaining second-order critical points for nonconvex finite-sums (1). This does
 465 not necessarily imply low test error or good generalization capabilities. Thus, we should be careful when
 466 interpreting the results presented in this paper. A detailed discussion or analysis of these issues is out of scope
 467 of this paper. While a few prior works argue for convergence to local optima, the exact connection between
 468 generalization and local optima is not well understood, and is an interesting open problem. Nevertheless, we
 469 believe the techniques presented in this paper can be used alongside other optimization tools for faster and
 470 better nonconvex optimization.